Journal of Applied and Computational Mechanics, Vol. 2, No. 4, (2016), 208-221

Journal of
Applied and Computational Mechanics

Nonlinear vibration analysis of single-walled carbon nanotube conveying fluid with slip boundary conditions using variational iterative method

Gbeminiyi M. Sobamowo

Department of Mechanical Engineering, University of Lagos, Akoka, Lagos, Nigeria.

Received November 05 2016; revised December 12 2016; accepted for publication December 20 2016.
Corresponding author: Gbeminiyi M. Sobamowo, mikegbeminiyiprof@yahoo.com

Abstract

In this paper, nonlinear dynamic behaviour of carbon nanotube conveying fluid with slip boundary conditions is studied using variation iteration method. The developed solutions are used to investigate the effects of various parameters on the nonlinear vibration of the nanotube. From the result, it is observed that increase in the slip parameter leads to decrease in the frequency of vibration and the critical velocity while natural frequency and the critical fluid velocity increase as the stretching effect increases. Also, as the nonlocal parameter increased, the natural frequency and the critical velocity decreased. The analytical solutions help to have better insights and understand the relationship between the physical quantities of the problem.

Keywords: Non-linear Vibration; Slip boundary Condition;Fluid-conveying Nanotube; Variational iteration method.

1. Introduction

Following the discovery of nanotube by Iijima [1], there have been rapid developments of nanotechnology due to the unique mechanical, thermal, chemical, electrical, electrochemical and electronic properties of carbon nanotube (CNT). As part of the numerous applications of CNT, it has been used for conveying/transporting fluid and the study of effects and the conditions of moving fluid on the overall mechanical behaviour of CNTs have of area that has aroused significant and challenging research interests. Consequently, the dynamic analysis of flow-induced vibration of CNT has has attracted a large number of studies in literatures in recent years [2-9]. Modeling the dynamic behaviours of the structures under the influence of some thermo-fluidic or thermo-mechanical parameters often results in nonlinear equations and such are difficult to find the exact analytical solutions. In some cases where decomposition procedures into spatial and temporal parts are carried out, the resulting nonlinear equation for the temporal part comes in form of Duffing equation. Application of analytical methods such as Exp-function method, He's Exp-function method, improved F-expansion method, Lindstedt-Poincare techniques, quotient trigonometric function expansion method to the nonlinear equation present analytical solutions either in implicit or explicit form which often involved complex mathematical analysis leading to analytic expression involving a large number terms. Furthermore, the methods are time-consuming task accompanied with possessing high skills in mathematics. Also, they do not provide general analytical solutions since the solutions often come with conditional statements which make them limited in used as many of the conditions with the exact solutions do not meet up with the practical applications. In practice, analytical solutions with large number of terms and conditional statements for the solutions are not convenient for use by designers and engineers [10]. Consequently, recourse has always been made to numerical methods or approximate analytical methods in solving the problems. However, the classical way for finding analytical solution is obviously still very important since it serves as an accurate benchmark for numerical solutions. Also, the experimental data are useful to access the mathematical models, but are never sufficient to verify the numerical solutions of the established mathematical models. Comparison between the numerical calculations and experimental data often fail to reveal the compensation of modelling deficiencies through the computational errors or unconscious approximations in establishing applicable numerical schemes. Additionally, analytical solutions for

specified problems are also essential for the development of efficient applied numerical simulation tools. Inevitably, exact analytical expressions are required to show the direct relationship between the models parameters. When such analytical solutions are available, they provide good insights into the significance of various system parameters affecting the phenomena as it gives continuous physical insights than pure numerical or computation methods. Furthermore, most of the analytical approximation and purely numerical methods that were applied in literatures to nonlinear problems are computationally intensive. Analytical expression is more convenient for engineering calculations compare with experimental or numerical studies and it is obvious starting point for a better understanding of the relationship between physical quantities/properties. It is convenient for parametric studies, accounting for the physics of the problem. It appears more appealing than the numerical solution as it helps to reduce the computation costs, simulations and task in the analysis of real life problems. Therefore, an exact analytical solution is required for the problem. Although, different approximate analytical methods such as Perturbation method (regular or singular perturbation method), Homotopy perturbation method (HPM), Homotopy analysis method (HAM), variational iterative method (VIM), differential transformation method (DTM), Harmonic balancing method, Adomian decomposition method etc. [11-15]. These approximate analytical methods solve nonlinear differential equations without linearization, without discretization or approximation of the derivatives. However, most of the approximate methods give accurate predictions only when the nonlinearities are weak and they fail to predict accurate solutions for strong nonlinear models. Also, when they are routinely implemented, they can sometimes lead to erroneous results [15]. Additionally, some of them require more mathematical manipulations and are not applicable to all problems, and thus suffer a lack of generality. For example, DTM proved to be more effective than most of the other approximate analytical solutions as it does not require many computations as carried out in ADM, HAM, HPM, and VIM. However, the transformation of the nonlinear equations and the development of equivalent recurrence equations for the nonlinear equations using DTM proved somehow difficult in some nonlinear system such as in rational Duffing oscillator, irrational nonlinear Duffing oscillator, finite extensibility nonlinear oscillator. Moreover, the determination of Adomian polynomials as carried out in ADM, the restrictions of HPM to weakly nonlinear problems, the lack of rigorous theories or proper guidance for choosing initial approximation, auxiliary linear operators, auxiliary functions, and auxiliary parameters in HAM, operational restrictions to small domains and the search for a particular value for the auxiliary parameter that will satisfy second the boundary condition which leads to additional computational cost in using DTM. Therefore, the quest for comparatively simple, flexible, generic and high accurate analytical solutions continues. In this work, variation iteration method (VIM) is used to develop approximate analytical solutions to nonlinear vibration analysis of single-walled carbon nanotube under the slip effects. Variational iteration method has shown to be the one of the most effective, accurate, convenient approximate analytical methods for large class of weakly and strongly nonlinear equations. It is a user friendly method with reduced size of calculation, direct and straightforward iteration and generates solution with a rapid rate of convergent and without any restrictive assumptions or transformations. In VIM, the initial solution can be freely chosen with some unknown parameters and the unknown parameters in the initial solution can be achieved easily. Although, there is a rigour of step-by-step integrations coupled with the problem of determination of Langrange multiplier in application of VIM, with few number of iteration, even, in some cases, a single iteration of VIM can converge to correct solutions or results. The analytical solutions as developed in this work can serve as a starting point for a better understanding of the relationship between the physical quantities of the problems as it provides continuous physical insights into the problem than pure numerical or computation methods.

2. Problem formulation based on nonlocal beam theory

Consider a carbon nanotube (CNT) conveying fluid as shown in Fig. 1.Based on the Eringen's nonlocal elasticity theory [16-19], the stress at a reference point x in an elastic continuum not only depends on the strain field at the same point but also in the strains at all other points of the body. Therefore, the equation for the linear homogeneous isotropic and nonlocal elastic solids with zero body force are given as

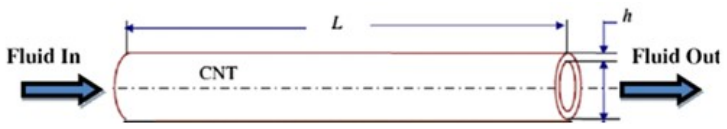

Fig. 1. a carbon nanotube (CNT) conveying fluid

$$\sigma_{ij} = 0 \tag{1}$$

$$\sigma_{ij}(x) = \int_V K\left(|x - x'|, \gamma\right) C_{ijkl}\varepsilon_{kl}(x')dV(x') \tag{2}$$

$$\varepsilon_{ij} = \frac{1}{2}\left(u_{ij} + u_{ji}\right) \tag{3}$$

It can easily be seen that it is very difficult to solve the elasticity problems by using the integral constitutive relation as given by Eq. (2). Consequently, an alternative and simplified constitutive relation in a differential form is

given by Eringen [16-19] as follows

$$\left(1-\left(e_o a\right)^2 \nabla^2\right)\sigma = T \tag{4}$$

For a nanotube (considering the small-size relation based effect), the nonlocal constitutive relation based on one-dimension equation of Eringen's nonlocal theory for the Euler-Bernoulli beam is given by

$$\sigma_{xx} - \left(e_o a\right)^2 \frac{\partial^2 \sigma_{xx}}{\partial x^2} = E\,\varepsilon_{xx} \tag{5}$$

Also, the internal moment for the Euler-Bernoulli beam is given as

$$T(x,t) = \int_A z\,\sigma_{xx}\,dA \tag{6}$$

where A is the cross sectional area of the nanotube. On substituting σ_{xx} from Eq. (5) into Eq. (6), we have [20]

$$T(x,t) = \left(e_o a\right)^2 \frac{\partial^2 T}{\partial x^2} - EI\,\frac{\partial^2 w}{\partial x^2} \tag{7}$$

On incorporating von Karman's nonlinearity, the internal shear force on the structural cross section must satisfy the moment equilibrium relation

$$Q(x,t) = \frac{\partial T}{\partial x} + N(x,t)\frac{\partial w}{\partial x} \tag{8}$$

It should be pointed out that the internal membrane force, N is constant along the beam as

$$\frac{\partial N}{\partial x} = 0 \quad \Rightarrow N(x,t) = N(t) \tag{9}$$

Therefore, Eq. (9) becomes

$$Q(x,t) = \frac{\partial T}{\partial x} + N(t)\frac{\partial w}{\partial x} \tag{10}$$

Differentiating Eq. (10) with respect to spatial variable x considering the absence of external axial load on the beam

$$\frac{\partial^2 T}{\partial x^2} = \frac{\partial Q}{\partial x} - N(t)\frac{\partial^2 w}{\partial x^2} \tag{11}$$

The differential equation of motion for the free vibration of the fluid-conveying nanotube can be expressed as

$$\frac{\partial Q}{\partial x} = m_c\,\frac{\partial^2 w}{\partial t^2} + F_w \tag{12}$$

m_c is the mass per unit length of the CNT and F_w is the force external by the fluid on beam structure, which can be expressed as

$$F_w = m_f\left(2v\,\frac{\partial^2 w}{\partial x\,\partial t} + v^2\,\frac{\partial^2 w}{\partial x^2} + \frac{\partial^2 w}{\partial t^2}\right) \tag{13}$$

Therefore,

$$\frac{\partial Q}{\partial x} = m_c\,\frac{\partial^2 w}{\partial t^2} + m_f\left(2v\,\frac{\partial^2 w}{\partial x\,\partial t} + v^2\,\frac{\partial^2 w}{\partial x^2} + \frac{\partial^2 w}{\partial t^2}\right) \tag{14}$$

Substituting Eq. (14) into Eq. (11), we have

$$\frac{\partial^2 T}{\partial x^2} = m_c \frac{\partial^2 w}{\partial t^2} + m_f \left(2v \frac{\partial^2 w}{\partial x \partial t} + v^2 \frac{\partial^2 w}{\partial x^2} + \frac{\partial^2 w}{\partial t^2} \right) - N(t) \frac{\partial^2 w}{\partial x^2} \tag{15}$$

For the immovable supports, the internal membrane force is given as

$$N(t) = \frac{EA}{2L} \int_0^L \left(\frac{\partial w}{\partial x} \right)^2 dx \tag{16}$$

Therefore, eq. (15) can be expressed

$$\frac{\partial^2 T}{\partial x^2} = m_c \frac{\partial^2 w}{\partial t^2} + m_f \left(2v \frac{\partial^2 w}{\partial x \partial t} + v^2 \frac{\partial^2 w}{\partial x^2} + \frac{\partial^2 w}{\partial t^2} \right) - \left[\frac{EA}{2L} \int_0^L \left(\frac{\partial w}{\partial x} \right)^2 dx \right] \frac{\partial^2 w}{\partial x^2} \tag{17}$$

If we substitute Eq. (17) into Eq. (7), we obtained

$$T(x,t) = \left(e_o a\right)^2 \left[m_c \frac{\partial^2 w}{\partial t^2} + m_f \left(2v \frac{\partial^2 w}{\partial x \partial t} + v^2 \frac{\partial^2 w}{\partial x^2} + \frac{\partial^2 w}{\partial t^2} \right) - \left[\frac{EA}{2L} \int_0^L \left(\frac{\partial w}{\partial x} \right)^2 dx \right] \frac{\partial^2 w}{\partial x^2} \right] - EI \frac{\partial^2 w}{\partial x^2} \tag{18}$$

Using Hamilton's principle gives

$$\begin{aligned} R(x,t) = {} & \frac{1}{2} \int_0^L m_c \left(\frac{\partial w}{\partial t} \right)^2 dx + \frac{1}{2} \int_0^L \left\{ \left(e_o a\right)^2 \left[\begin{array}{l} m_c \frac{\partial^2 w}{\partial t^2} + m_f \left(2v \frac{\partial^2 w}{\partial x \partial t} + v^2 \frac{\partial^2 w}{\partial x^2} + \frac{\partial^2 w}{\partial t^2} \right) \\ - \left[\frac{EA}{2L} \int_0^L \left(\frac{\partial w}{\partial x} \right)^2 dx \right] \frac{\partial^2 w}{\partial x^2} \end{array} \right] - EI \frac{\partial^2 w}{\partial x^2} \right\} \frac{\partial^2 w}{\partial x^2} dx \\ & - \frac{1}{2} \int_0^L \left[\frac{EA}{2L} \int_0^L \left(\frac{\partial w}{\partial x} \right)^2 dx \right] \left(\frac{\partial w}{\partial x} \right)^2 dx \end{aligned} \tag{19}$$

In Eq. (19), the first integral is the kinetic energy of the nanotube while the second integral represents the elastic energy induced by the bending and the third integral is the elastic energy in extension due to stretching of the neutral axis. From Eq. (19), the nonlinear partial-differential equation of the CNT conveying fluid is expressed as

$$\begin{aligned} R(x,t) = {} & EI \frac{\partial^4 w}{\partial x^4} + m \frac{\partial^2 w}{\partial t^2} + 2v m_f \frac{\partial^2 w}{\partial x \partial t} + m_f v^2 \frac{\partial^2 w}{\partial x^2} - \left[\frac{EA}{2L} \int_0^L \left(\frac{\partial w}{\partial x} \right)^2 dx \right] \frac{\partial^2 w}{\partial x^2} \\ & - \left(e_o a\right)^2 \left[m \frac{\partial^4 w}{\partial x^2 \partial t^2} + 2v m_f \frac{\partial^4 w}{\partial x^3 \partial t} + m_f v^2 \frac{\partial^4 w}{\partial x^4} - \left[\frac{EA}{2L} \int_0^L \left(\frac{\partial w}{\partial x} \right)^2 dx \right] \frac{\partial^4 w}{\partial x^4} \right] = 0 \end{aligned} \tag{20}$$

For the simply support beam considered in this study, the initial and the boundary conditions are

$$\begin{aligned} & w(0,x) = A \;\; \dot{w}(0,x) = 0 \\ & w(0,t) = w''(0,t) = 0 \;\; w(L,t) = w''(L,t) = 0 \end{aligned} \tag{21}$$

If stretching effect in the nanotube is neglected in the Eq. (20), we recovered the classical governing equation for flow-induced vibration of fluid-conveying in nanotube

$$EI \frac{\partial^4 w}{\partial x^4} + m \frac{\partial^2 w}{\partial t^2} + 2v m_f \frac{\partial^2 w}{\partial x \partial t} + m_f v^2 \frac{\partial^2 w}{\partial x^2} - \left(e_o a\right)^2 \left[m \frac{\partial^4 w}{\partial x^2 \partial t^2} + 2v m_f \frac{\partial^4 w}{\partial x^3 \partial t} + m_f v^2 \frac{\partial^4 w}{\partial x^4} \right] = 0 \tag{22}$$

where the natural frequency gives

$$\omega_n = \left(\frac{n\pi}{L}\right)^2 \sqrt{\frac{EI}{m\left\{1+\left((e_o a)\frac{n\pi}{L}\right)^2\right\}}} \tag{23}$$

If the nano-size and stretching effects are neglected in the eq. (20), we have

$$EI\frac{\partial^4 w}{\partial x^4} + m\frac{\partial^2 w}{\partial t^2} + 2vm_f\frac{\partial^2 w}{\partial x\,\partial t} + m_f v^2\frac{\partial^2 w}{\partial x^2} = 0 \tag{24}$$

which is the classical governing equation for flow-induced vibration of fluid-conveying pipe; where the natural frequency gives

$$\omega_n = \left(\frac{n\pi}{L}\right)^2 \sqrt{\frac{EI}{m}} \tag{25}$$

For CBT conveying fluid, the radius of the tube is assumed to be the characteristics length scale, Knudsen number is larger than 10^{-2}. Therefore, the assumption of no-slip boundary conditions does not hold and modified model should be used.

$$VCF = \frac{U_{avg,slip}}{U_{avg,no-slip}} = \left(1+a_k Kn\right)\left[4\left(\frac{2-\sigma_v}{\sigma_v}\right)\left(\frac{Kn}{1+Kn}\right)+1\right] \tag{26}$$

Where Kn is the Knudsen number, σ_v is tangential moment accommodation coefficient which is considered to be 0.7 for most practical purposes [21].

$$a_k = a_o\frac{2}{\pi}\left[tan^{-1}\left(a_1 Kn^B\right)\right] \tag{27}$$

$$a_o = \frac{64}{3\pi\left(1-\frac{4}{b}\right)} \tag{28}$$

Therefore,

$$U_{avg,slip} = \left(1+a_k Kn\right)\left[4\left(\frac{2-\sigma_v}{\sigma_v}\right)\left(\frac{Kn}{1+Kn}\right)+1\right]U_{avg,no-slip} = VCF\left(U_{avg,no-slip}\right) \tag{29}$$

And Eq. (20) could be written as

$$\begin{aligned} R(x,t) = {} & EI\frac{\partial^4 w}{\partial x^4} + m\frac{\partial^2 w}{\partial t^2} + 2m_f\left[VCF\left(U_{avg,no-slip}\right)\right]\frac{\partial^2 w}{\partial x\,\partial t} \\ & + m_f\left[VCF\left(U_{avg,no-slip}\right)\right]^2\frac{\partial^2 w}{\partial x^2} - \left[\frac{EA}{2L}\int_0^L\left(\frac{\partial w}{\partial x}\right)^2 dx\right]\frac{\partial^2 w}{\partial x^2} \\ & -(e_o a)^2\left[\begin{array}{l} m\dfrac{\partial^4 w}{\partial x^2\partial t^2} + 2m_f\left[VCF\left(U_{avg,no-slip}\right)\right]\dfrac{\partial^4 w}{\partial x^3\partial t} \\ +m_f\left[VCF\left(U_{avg,no-slip}\right)\right]^2\dfrac{\partial^4 w}{\partial x^4} - \left[\dfrac{EA}{2L}\displaystyle\int_0^L\left(\dfrac{\partial w}{\partial x}\right)^2 dx\right]\dfrac{\partial^4 w}{\partial x^4} \end{array}\right] = 0 \end{aligned} \tag{30}$$

Using the Galerkin's decomposition procedure to separate the spatial and temporal parts of the lateral displacement functions as

$$w(x,t) = \phi(x)u(t) \tag{31}$$

Where $u(t)$ the generalized coordinate of the system and $\phi(x)$ is a trial/comparison function that will satisfy both the geometric and natural boundary conditions.

Applying one-parameter Galerkin's solution given in Eq. (31) to Eq. (30)

$$\int_0^L R(x,t)\phi(x)dx \tag{32}$$

Where

$$\begin{aligned} R(x,t) &= EI\frac{\partial^4 w}{\partial x^4} + m\frac{\partial^2 w}{\partial t^2} + 2m_f\left[VCF\left(U_{avg,no-slip}\right)\right]\frac{\partial^2 w}{\partial x\,\partial t} \\ &+ m_f\left[VCF\left(U_{avg,no-slip}\right)\right]^2\frac{\partial^2 w}{\partial x^2} - \left[\frac{EA}{2L}\int_0^L\left(\frac{\partial w}{\partial x}\right)^2 dx\right]\frac{\partial^2 w}{\partial x^2} \\ &-(e_o a)^2\left[\begin{array}{l} m\dfrac{\partial^4 w}{\partial x^2\partial t^2} + 2m_f\left[VCF\left(U_{avg,no-slip}\right)\right]\dfrac{\partial^4 w}{\partial x^3\partial t} \\ +m_f\left[VCF\left(U_{avg,no-slip}\right)\right]^2\dfrac{\partial^4 w}{\partial x^4} - \left[\dfrac{EA}{2L}\displaystyle\int_0^L\left(\dfrac{\partial w}{\partial x}\right)^2 dx\right]\dfrac{\partial^4 w}{\partial x^4} \end{array}\right] = 0 \end{aligned} \tag{33}$$

For the simply-supported nanotube

$$\phi(x) = \sin\beta_n x \tag{34}$$

where

$$\sin\beta_n L = 0 \quad \Rightarrow \beta_n = \frac{n\pi}{L} \quad n=1, 2, 3, 4....$$

We arrived at

$$M\ddot{u}_s(t) + G\dot{u}_s(t) + (K+C)u_s(t) - Vu_s^3(t) = 0 \tag{35}$$

where

$$u_s = VCF\left(U_{avg,no-slip}\right)$$

$$M = \int_0^L (m_p + m_f)\phi(x)\left(\phi(x) - (e_o a)^2\frac{d^2\phi}{dx^2}\right)dx$$

$$G = \int_0^L \phi(x)\left\{2m_f u_s\left(\frac{d\phi}{dx} - (e_o a)^2\frac{d^3\phi}{dx^3}\right)\right\}dx$$

$$K = \int_0^L EI\,\phi(x)\frac{d^4\phi}{dx^4}dx$$

$$C = \int_0^L m_f u_s^2\phi(x)\left(\frac{d^2\phi}{dx^2} - (e_o a)^2\frac{d^4\phi}{dx^4}\right)dx$$

$$V = \int_0^L \frac{EA}{2L}\phi(x)\left\{\left[\int_0^L\left(\frac{\partial\phi}{\partial x}\right)^2 dx\right] - \left\{\frac{d^2\phi}{dx^2} - (e_o a)^2\frac{d^4\phi}{dx^4}\right\}\right\}dx$$

Under the transformation, $\tau = \omega t$, Eq. (35) turns out to be

$$M\omega^2\ddot{u}(\tau) + G\omega\dot{u}(\tau) + (K+C)u(\tau) - Vu^3(\tau) = 0 \tag{36a}$$

For the undamped simple-simple supported structures, *G = 0*

$$M\omega^2\ddot{u}(\tau)+(K+C)u(\tau)-Vu^3(\tau)=0 \tag{36b}$$

3. Method of solution: Variational iteration method

It is very difficult to generate any closed form solution for the above nonlinear simultaneous Eqs. (36). However, a closed form series solution or approximate analytical solution can be obtained for the non-linear differential equations. In finding direct and practical solutions to the problem, variational iteration method is applied to nonlinear equations. As pointed previously, the variational iteration method is an approximate analytical method for solving differential equations. The basic definitions of the method are as follows

The differential equation to be solved can be written in the form

$$Lu+Nu=g(t) \tag{37}$$

Where L is a linear operator, N is a nonlinear operator and $g(t)$ is an inhomogeneous term in the differential equation.

Following VIM procedure, we have a correction functional as

$$u_{n+1}(t)=u_n(t)+\int_0^t\lambda\left\{Lu_n(\tau)+N\tilde{u}(\tau)-g(t)\right\}d\tau \tag{38}$$

λ is a general Langrange multiplier, the subscript n is the nth approximation and $\tilde{u}$ is a restricted variation $\delta\tilde{u}=0$. Making the above correction functional stationary and also, consider $\delta u_{n+1}=0$, we have

$$\delta u_{n+1}(t)=\delta u_n(t)+\lambda(\delta u_n)'\Big|_0^t-\lambda'(\delta u_n)'\Big|_0^t+\int_0^t\left\{\lambda''+\lambda\left(\frac{K+C}{M}\right)\right\}\delta u_n d\tau=0 \tag{39}$$

Where its stationary conditions are

$$\begin{aligned}&1-\lambda'(\tau)\big|_{\tau=t}=0\\&\lambda(\tau)\big|_{\tau=t}=0\\&\lambda''(\tau)+\left(\frac{K+C}{M}\right)\lambda(\tau)=0\end{aligned} \tag{40}$$

On solving the above Eq. (40), we have a Langrange multiplier as

$$\lambda(\tau)=\sqrt{\frac{M}{K+C}}\int_0^t sin\left\{\sqrt{\frac{K+C}{M}}(\tau-t)\right\} \tag{41}$$

Therefore, Eq. (38) can be written as

$$u_{n+1}=u_n+\sqrt{\frac{M}{K+C}}\int_0^t sin\left\{\sqrt{\frac{K+C}{M}}(\tau-t)\right\}\left\{M\omega^2\frac{d^2u_n}{d\tau^2}+(K+C)u_n-Vu_n^3\right\}d\tau \tag{42}$$

In order to find the periodic solution of Eq. (42), assume an initial approximation for zero-order deformation to be

$$u_o(\tau)=A\cos\tau \tag{43}$$

Then residual is given as

$$R(\tau) = -M\omega_o^2 A\cos\tau + (K+C)A\cos\tau - VA^3\cos^3\tau \tag{44}$$

Which is also

$$R(\tau) = -M\omega^2 A\cos\tau + (K+C)A\cos\tau - VA^3\left(\frac{3\cos\tau+\cos 3\tau}{4}\right) \tag{45}$$

Collecting like terms at the RHS

$$R(\tau) = \left((K+C)A - \frac{3VA^3}{4} - M\omega^2 A\right)\cos\tau - \frac{1}{4}VA^3\cos 3\tau \tag{46}$$

In order to eliminate the secular term, the coefficient of $\cos\tau$ must vanish. Therefore,

$$\left((K+C)A - \frac{3VA^3}{4} - M\omega_o^2 A\right) = 0 \tag{47}$$

Thus, for the zero-order nonlinear natural frequency, we have

$$\omega_o \approx \sqrt{\frac{K+C}{M} - \frac{3VA^2}{4M}} \tag{48}$$

Therefore, the ratio of the zero-order nonlinear natural frequency, ω_o to the linear frequency, ω_b

$$\frac{\omega_o}{\omega_b} \approx \sqrt{1 - \frac{3VA^2}{4(K+C)}} \tag{49}$$

where

$$\omega_b = \sqrt{\frac{K+C}{M}}$$

Similarly, for the first-order nonlinear natural frequency, we have

$$\omega_1 \approx \sqrt{\frac{1}{2}\left\{\left[\left(\frac{K+C}{M}\right) - \left(\frac{3VA^2}{4M}\right)\right] + \sqrt{\left[\left(\frac{K+C}{M}\right) - \left(\frac{3VA^2}{4M}\right)\right]^2 - \left(\frac{3V^2A^4}{32M^2}\right)}\right\}} \tag{50}$$

The ratio of the first-order nonlinear frequency, ω_1 to the linear frequency, ω_b

$$\frac{\omega_1}{\omega_b} \approx \sqrt{\frac{1}{2}\left\{\left[1 - \left(\frac{3VA^2}{4(K+C)}\right)\right] + \sqrt{\left[1 - \left(\frac{3VA^2}{4(K+C)}\right)\right]^2 - \left(\frac{3V^2A^4}{32(K+C)}\right)}\right\}} \tag{51}$$

For the first iteration,

$$u_1 = u_0 + \int_0^t \lambda(\tau)R_0(\tau)d\tau \tag{52}$$

Substitute Eqs. (41), (43) and (46) in Eq. (52) , we have

$$u_1 = u_0 + \sqrt{\frac{M}{K+C}}\int_0^t \sin\left\{\sqrt{\frac{K+C}{M}}(\tau - t)\right\}\left\{M\omega^2\ddot{u}_0 + (K+C)u_0 - Vu_0^3\right\}d\tau \tag{53}$$

Substitute Eqs. (43) in Eq.(53) , we have

$$u_1 = A\cos\tau + \sqrt{\frac{M}{K+C}}\int_0^t \sin\left\{\sqrt{\frac{K+C}{M}}(\tau - t)\right\}\left\{-M\omega_o^2 A\cos\tau + (K+C)A\cos\tau - VA^3\cos^3\tau\right\}d\tau \tag{54}$$

A further simplification gives

$$u_1 = \frac{K+C}{9M\omega^2 - K + C}\left\{\frac{9AM\omega^2}{K+C}\cos\tau - A\cos\tau - \frac{A^3}{16}\cos\tau + \frac{A^3}{16}\cos(3\tau)\right\} \tag{55}$$

Which can be written as

$$u(t) \approx \left(\frac{K+C}{9M\omega^2 - K + C}\right)\left\{\frac{9AM\omega^2}{K+C}\cos(\omega t) - A\cos(\omega t) - \frac{A^3}{16}\cos(\omega t) + \frac{A^3}{16}\cos(3\omega t)\right\} \tag{56}$$

Substitute Eqs. (34) and (56) into Eq. (32), we have

$$w(x,t) \approx \left(\frac{K+C}{9M\omega^2 - K + C}\right)\left\{\frac{9AM\omega^2}{K+C}\cos(\omega t) - A\cos(\omega t) - \frac{A^3}{16}\cos(\omega t) + \frac{A^3}{16}\cos(3\omega t)\right\}\sin\frac{n\pi x}{L} \tag{57}$$

where

$$\omega \approx \sqrt{\frac{1}{2}\left\{\left[\left(\frac{K+C}{M}\right) - \left(\frac{3VA^2}{4M}\right)\right] + \sqrt{\left[\left(\frac{K+C}{M}\right) - \left(\frac{3VA^2}{4M}\right)\right]^2 - \left(\frac{3V^2A^4}{32M^2}\right)}\right\}}$$

It can easily be seen that as the nonlinear term tends to zero, the frequency ratio of the nonlinear frequency to the linear frequency, $\frac{\omega}{\omega_b}$ tends to 1.

$$\lim_{\xi_2 \to 0}\frac{\omega}{\omega_b} = 1 \tag{58}$$

Also, as the amplitude A tends to zero, the frequency ratio of the nonlinear frequency to the linear frequency, $\frac{\omega}{\omega_b}$ tends to 1.

$$\lim_{A \to 0}\frac{\omega}{\omega_b} = 1 \tag{59}$$

For very large values of the amplitude A, we have

$$\lim_{A \to \infty}\frac{\omega}{\omega_b} = \infty \tag{60}$$

4. Results and Discussion

The first five normalized mode shapes of the beams simple-simple are shown in Fig. 2. Also, the figure shows the deflections of the beam along the beams' span at five different buckled and mode shapes.

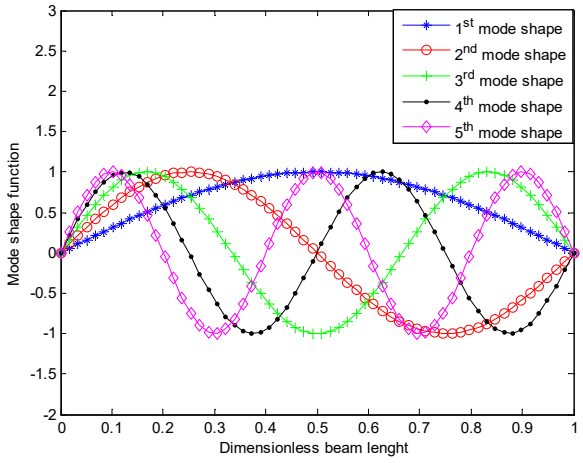

Fig. 2. The first five normalized mode shaped of the under simple supports nanotube

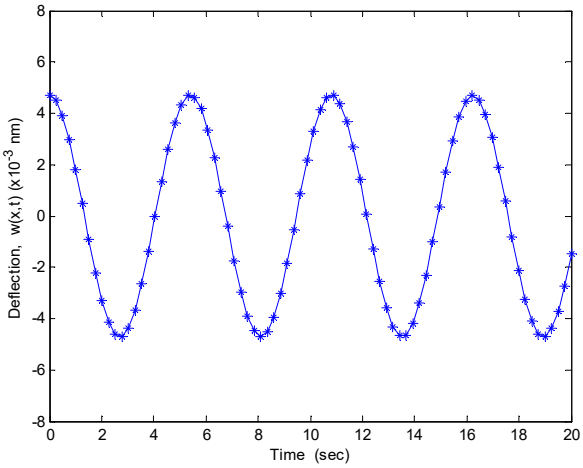

Fig. 3. Midpoint deflection time history for the nonlinear analysis of SWCBT when Kn=0.03 and U= 100 m/s

Effects of slip parameter called Knudsen number and the fluid flow velocity on the deflection of the the nanotube are presented in Fig. 3-5. Fig. 3 illustrates the midpoint deflection time history for the nonlinear analysis of SWCBT when *Kn = 0.03* and *U= 100 m/s* while Fig. 4 presents the midpoint deflection time history for the nonlinear analysis of SWCBT when *Kn = 0.03* and *U= 500 m/s*. Also, Fig. 5 depicts the midpoint deflection time history for the nonlinear analysis of SWCBT when *Kn = 0.1* and *U= 500 m/s* while Fig. 6 shows the midpoint deflection time history when *Kn = 0.05*, *U= 500 m/s*and when *Kn = 0.1* and *U= 500 m/s,* respectively. Fig. 7 shows the comparison of the linear vibration with nonlinear vibration of the SWCNT. It could be seen in the figure that the discrepancy between the linear and nonlinear amplitudes increases with increment of the maximum vibration. These results are in line with the results of Ali-Asgari*et al.* [20].

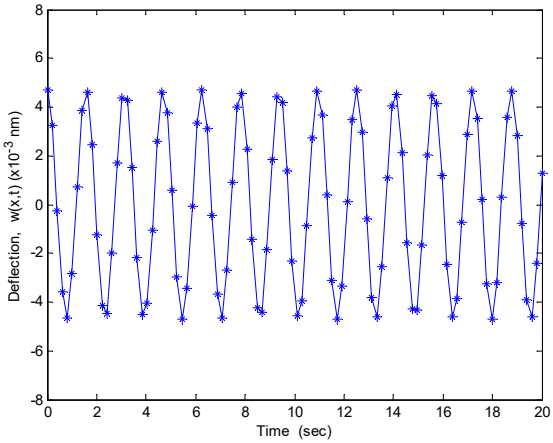

Fig. 4. Midpoint deflection time history for the nonlinear analysis of SWCBT when Kn=0.03 and U= 500 m/s

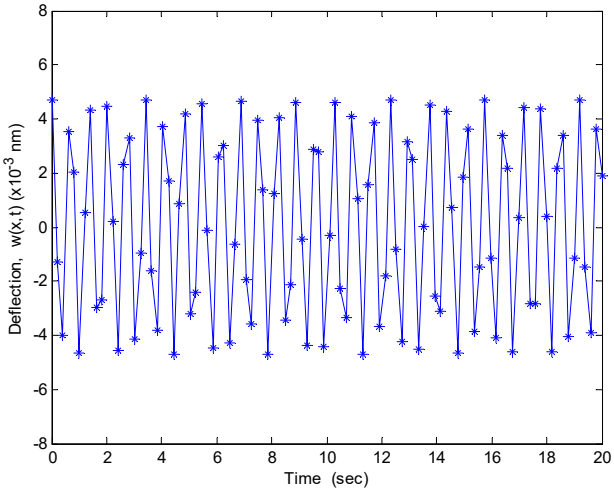

Fig. 6. Midpoint deflection time history for the linear analysis of SWCBT when Kn=0.1 and U= 500 m/s

Effects of slip parameter, Knudsen number on the dimensionless frequency ratio of the nanotube are shown in Figs. 8. It is depicted that increase in the slip parameter leads to decrease in the dimensionless frequency ratio of vibration of the SWCNT. It should be pointed out that the Knudsen number predicts various flow regimes in the fluid-conveying nanotube. The Knudsen number with zero value has the highest frequency as shown in the figure. As the Knudsen number increases, the bending stiffness of the nanotube decreases and in consequent, the critical continuum flow velocity decreases as the curves shift to the lowest frequency zone.

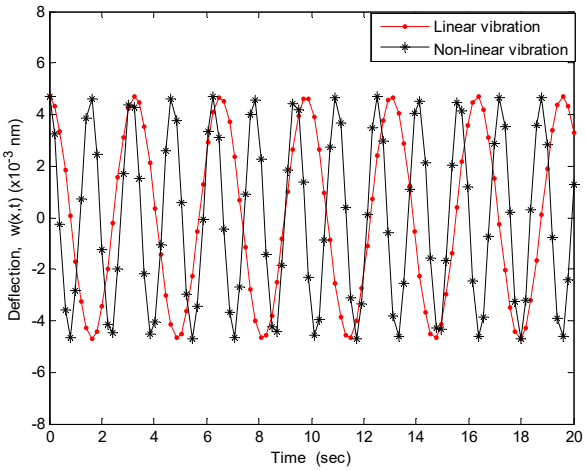

Fig. 7. Comparison of midpoint deflection time history for the linear and nonlinear analysis of CBT when Kn=0.03 and U= 500 m/s

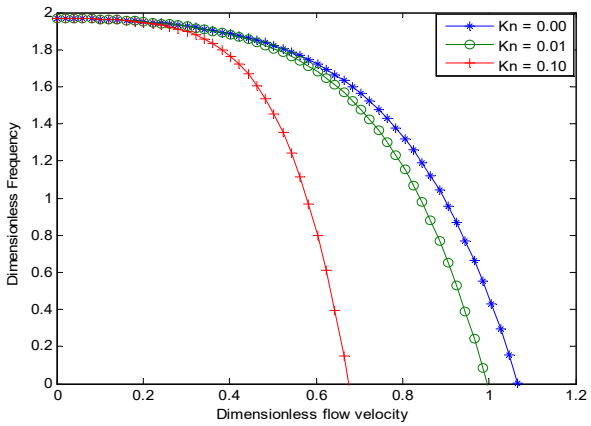

Fig. 8. Effects of Knudsen number on the dimensionless frequency of simply supported single-walled nanotube

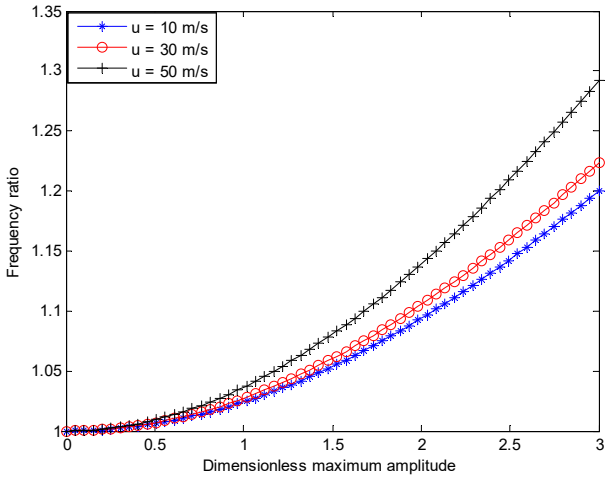

Fig. 9. Effects of fluid-flow velocity on the nonlinear amplitude-frequency response curves of the nanotube

Fig. 9 shows the effects of fluid-flow velocity on the nonlinear amplitude-frequency response curves of nanotube. It is observed that as the fluid-flow velocity increases, the nonlinear vibration frequency ratio increases and the difference between the nonlinear and linear frequency becomes pronounced. The results in Figs. 9 reveal that fluid flow velocity has significant effects on the nonlinear behaviour of the nanotube and therefore, this and other

significant parameters can be used to control the nonlinearity of the structure.

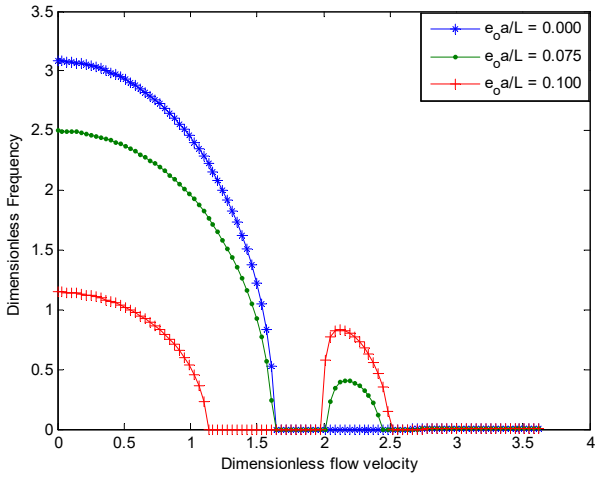

Fig. 10. Effects of nonlocal parameter on the natural frequency of the nonlinear vibration

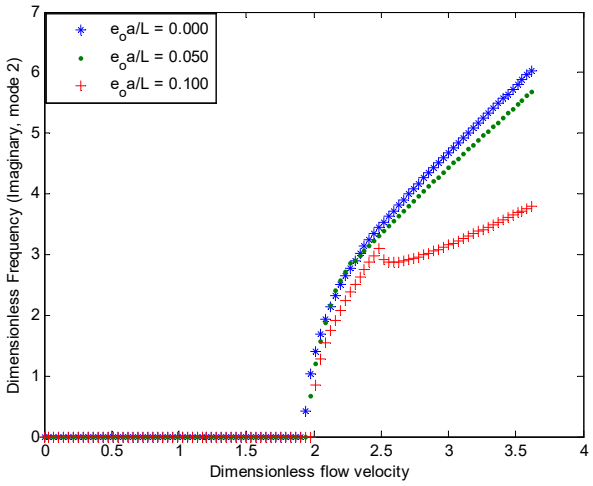

Fig. 11. Effects of nonlocal parameter on the natural frequency of the nonlinear vibration

The studies and the investigations of the dynamic and stability behaviours of the structure are largely dependent on the effects of fluid flow velocity and amplitude on the natural frequencies of the vibration. Effects of nonlocal parameter on the vibration of the nanotube are shown in Fig. 10-11. It is depicted that increase in the slip parameter leads to decrease in the frequency of vibration of the structure and the critical velocity of the conveyed fluid. It should be pointed out as shown in the figures that the zero value for the nonlocal parameter, i.e. $e_o a = 0$, represents the results of the classical Euler-Bernoulli model which has the highest frequency and critical fluid velocity (a point where the structure starts to experience instability). When the flow velocity of the fluid attains the critical velocity, both the real and imaginary parts of the frequency are equal to zero. Also, the figures present the critical speeds corresponding to the divergence conditions for different values of the nonlocal parameters. It is shown in Figs. 10 and 11, the real and imaginary parts of the eigenvalues related to the two lowest modes with different nanotube parameters.

7. Conclusion

In this work, analytical solutions have been provided to analyze the effects of slip boundary conditions on the nonlinear dynamic behaviours of carbon nanotube conveying fluid using variation iteration method. The results show that the alteration of nonlinear flow-induced frequency from linear frequency is significant as the amplitude, flow velocity, and aspect ratio increase. The analytical solutions can serve as benchmarks for other methods of solutions of the problem. They can also provide a starting point for a better understanding of the relationship between the physical quantities of the problems.

Nomenclature

A	Area of the structure
E	Young Modulus of Elasticity
I	moment of area

Kn	Knudsen number
l_o, l_1, l_2	independent length scale parameters
L	length
m_p	mass of the structure
m_f	mass of fluid
N	axial/Longitudinal force
r	radius of the structure
t	time
$u(t)$	generalized coordinate of the system
w	transverse displacement/deflection
x	axial coordinate
$Z_o(x)$	the arbitrary initial rise function
σ_v	tangential moment accommodation coefficient
$\phi(x)$	trial/comparison function
υ	Poisson' ratio
μ	damping coefficient

References

1. Iijima, S. Helical microtubules of graphitic carbon. Nature, London, Vol. 354, no. 6348, pp. 56–58, 1991.
2. Yoon, G., Ru, C.Q., Mioduchowski, A. Vibration and instability of carbon nanotubes conveying fluid. Journal of Applied Mechanics, Transactions of the ASME, Vol. 65, no. 9, 1326–1336, 2005.
3. Yan, Y., Wang, W.Q. and Zhang, L.X. Nonlocal effect on axially compressed buckling of triple-walled carbon nanotubes under temperature field. Journal of Applied Math and Modelling, Vol. 34, pp. 3422–3429, 2010.
4. Murmu, T., and Pradhan, S. C. Thermo-mechanical vibration of Single-walled carbon nanotube embedded in an elastic medium based on nonlocal elasticity theory. Computational Material Science, Vol. 46, pp. 854–859, 2009.
5. Yang, H. K. and Wang, X. Bending stability of multi-wall carbon nanotubes embedded in an elastic medium. Modeling and Simulation in Materials Sciences and Engineering, Vol. 14, pp. 99–116, 2006.
6. Yoon, J. Ru, C.Q., Mioduchowski, A. Vibration of an embedded multiwall carbon nanotube. Composites Science and Technology, Vol. 63, no. 11, pp. 1533–1542, 2003.
7. Lu, P. Lee, H.P., Lu, C. Zhang, P.Q. Application of nonlocal beam models for carbon nanotubes. International Journal of Solids and Structures, Vol. 44, no. 16, pp. 5289–5300, 2007.
8. Zhang, Y., Liu, G., Han, X. Transverse vibration of double-walled carbon nanotubes under compressive axial load. Applied Physics Letter A, Vol. 340, no. 1-4, pp. 258–266, 2005.
9. GhorbanpourArani, M.S. Zarei, M. Mohammadimehr, A. Arefmanesh, M.R. Mozdianfard. The thermal effect on buckling analysis of a DWCNT embedded on the Pasternak foundation", Physica E, Vol. 43, pp. 1642–1648, 2011.
10. Sobamowo, M. G. Thermal analysis of longitudinal fin with temperature-dependent properties and internal heat generation using Galerkin's method of weighted residual. Applied Thermal Engineering Vol. 99, pp.1316–1330, 2016.
11. Rafei, M. Ganji, D. D. Daniali, H., Pashaei. H. The variational iteration method for nonlinear oscillators with discontinuities. J. Sound Vib. Vol. 305, pp. 614–620, 2007.
12. S. S. Ganji, D. D. Ganji, D. D., H. Ganji, Babazadeh, Karimpour, S.: Variational approach method for nonlinear oscillations of the motion of a rigid rod rocking back and cubic-quintic duffing oscillators. Prog. Electromagn. Res. M Vol. 4, pp. 23–32, 2008.
13. Liao, S. J. The Proposed Homotopy Analysis Technique for the Solution of Nonlinear Problems,Ph. D. dissertation, Shanghai Jiao Tong University, 1992
14. Zhou, J. K. Differential Transformation and its Applications for Electrical Circuits. *Huazhong University Press: Wuhan, China,* 1986.
15. Fernandez, A. On some approximate methods for nonlinear models. Appl Math Comput., Vol. 21., pp. 168-74, 2009
16. Eringen, A. C. "On differential equations of nonlocal elasticity and solutions of screw dislocation and surface waves", Journal of Applied Physics, Vol. 54, no. 9, pp.4703–4710, 1983.
17. Eringen, A. C. "Linear theory of nonlocal elasticity and dispersion of plane waves", Inter- national Journal of Engineering Science, Vol. 10, no. (5), pp. 425–435, 1972.
18. Eringen, A. C. and Edelen, D. G., B. "On nonlocal elasticity", International Journal of Engineering Science, Vol. 10, no.(3), pp. 233–248, 1972.
19. Eringen, A. C. "Nonlocal continuum field theories", Springer, New York 2002.

20. Ali-Asgari, M., Mirdamadi, H. R. and Ghayour, M. Coupled effects of nano-size, stretching, and slip boundary conditions on nonlinear vibrations of nano-tube conveying fluid by the homotopy analysis method.Physica E, Vol. 52, pp. 77–85, 2013.
21. Shokouhmand, H. Isfahani, A. H. M. and Shirani, E. “Friction and heat transfer coefficient in micro and nano channels with porous media for wide range of Knudsen number”, International Communication in Heat and Mass Transfer, Vol. 37, pp. 890-894, 2010.